

LiDAR Simulation for Performance Evaluation of UAS Detect and Avoid

James Riordan
ALMADA Research Centre
School of Computing, Engineering, and Physical Science
University of the West of Scotland
Lanarkshire, Scotland
james.riordan@uws.ac.uk

Alexander Dow
ALMADA Research Centre
School of Computing, Engineering, and Physical Science
University of the West of Scotland

Manduhu Manduhu
ALMADA Research Centre
School of Computing, Engineering, and Physical Science
University of the West of Scotland
Lanarkshire, Scotland

Gerard Dooly
Centre for Robotics and Intelligent Systems
Department of Electronic and Computer Engineering
University of Limerick

Julie Black
ALMADA Research Centre
School of Computing, Engineering, and Physical Science
University of the West of Scotland

Santiago Matalonga
ALMADA Research Centre
School of Computing, Engineering, and Physical Science
University of the West of Scotland

Abstract— The solution to mitigating risks associated with beyond Visual Line of Sight (BVLOS) operations of Unmanned Aerial System (UAS) generally focuses on the use of advanced Unmanned Traffic Management (UTM) systems. However, this solution does not take into account other uncooperative objects in the airspace. A more robust approach is to have UTM integrations coupled with onboard machine vision which is tied to automated collision avoidance systems. Future BVLOS regulations in urban situations may require robust embedded software that is capable of detecting air collision hazards in real-time at near and far ranges as uncooperative small aircraft and other unpredictable small objects with fast-changing and unscheduled trajectories pose significant hazards to UAS. This work presents the concept and initial prototyping of a Digital Twin to evaluate the capability of UAS mounted LiDAR to detect small-object air collision risks. A Digital Twin of the Port of Hamburg is augmented with typical port and harbour aerial hazards such as birds, drones, helicopters, and low flying aircraft. The use case scenarios are created in Maya and Unity, with Optix ray tracing of typical LiDAR imaging configurations used to replicate the cause and effect relationship between different LiDAR specifications and their response to small flying objects. Our results demonstrate the inhomogeneous point clouds generated at different spatial-temporal parts of the LiDAR scanning cycle and field of view. These results confirm the challenges of detecting small uncooperative objects by LiDAR.

Keywords—unmanned aerial systems, detect and avoid, perception, data driven simulation

I. INTRODUCTION

Fully-autonomous and/or Beyond Visual Line of Sight (BVLOS) operation of Unmanned Aerial System (UAS) may only be achieved when they are able to comply with the requirements to Detect and Avoid (DAA) uncooperative ground and air collision hazards. Current UAS ground support platforms enable mission planning by establishing geo-fences and mandatory clearance heights around and above known built environment structures identified in 3D annotated maps. While trajectories of nearby cooperative air traffic is contained in real-time ADS-B tracking data, permitted UAS

flight volumes are bounded by low altitude ceilings that aids vertical separation from conventional air traffic. However, uncooperative small aircraft and unpredictable small objects with fast-changing and unscheduled trajectories pose significant air collision hazards within UAS flight corridors. UAS onboard capability to tactically sense and detect small air collision risks such as small aircraft, helicopters, birds, and recreational drones has not yet been validated. Even the most advanced UAS do not have certified functioning DAA and full compliance is unlikely in the near term [1]. Indeed the DAA requirements and standards have not yet been defined and regulatory bodies such as for example the European Union Aviation Safety Agency (EASA) do not recognise any experience with autonomous UAS operations [2].

The sensor options for onboard DAA are Light Detection and Ranging (LiDAR), RADio Detection And Ranging (RADAR), acoustic and camera (including thermal and hyperspectral), with LiDAR advantageously providing depth information and high resolution at range [3]. Current UAS mountable LiDAR are designed predominantly for mapping and inspection use cases, however LiDAR can potentially ensure safe avoidance of many classes of obstacles [4]. However, there are critical gaps between current UAS LiDAR capabilities and future full compliance. The validation of LiDAR-based DAA is a prerequisite to future UAS concepts that are oriented towards UAS swarms operating in populated urban and industrial use cases. While the built environment occludes long range visibility, short range air-air LiDAR provides the depth and resolution needed to detect small collision hazards in cluttered and unsegregated environments.

This paper presents our approach to determine and identify those gaps. By adapting high-performance LiDAR simulation towards data-driven validation of uncooperative small object detection, our objective is to improve current operational risk assessment and management by discovering sensor deficiencies and air surveillance vulnerabilities.

We present the scenario Digital Twin of an urban industrial maritime port, which we extend with support to model uncooperative air collision hazards using 3D modelling

and animation software Maya and game engine Unity. The virtual UAS is equipped with a reconfigurable LiDAR implemented by an Optix ray tracer. Models of typical port and harbour aerial hazards such as birds, drones, helicopters, and low flying aircraft are incorporated into the virtual theatre to challenge the LiDAR detection. Our results demonstrate the capability of the LiDAR simulator to replicate complex laser configurations and non-repetitive line scanning patterns. They show the inhomogeneous point clouds generated at different spatial-temporal parts of the LiDAR scanning cycle and field of view when imaging a typical railway bridge situation and encountering flight risk due to the presence of a flock of birds and small low flying aircraft. The results show that as the range increases images performance is degraded, rendering small uncooperative flying object practically unrecognisable.

II. PREVIOUS WORK

A. Standards for Detect and Avoid

DAA approaches are generally divided between cooperative approaches (e.g., Traffic Collision and Avoidance Systems, Mode-C/S, ADS-B) and non-cooperative approaches. Non-cooperative approaches include imaging LiDAR, RADAR, camera, and acoustic sensors, with a distinction between active/pассив and ground/airborne approaches [5]. UAS generally carry a range of imaging sensors that are mostly used as payloads for mapping and inspection, and not for navigation and control [6]. This poses many issues for BVLOS operations, as the UAS is not capable of reacting to unknown hazards in its environment. In the case of manned commercial flight or VLOS UAS operations, the onboard pilot can mitigate these scenarios and associated risks, averting incidents. If UAS are to become commonplace and accepted for BVLOS flight, the risk associated with these and similar scenarios needs to be addressed [7]. Emerging UAS regulatory and standards roadmaps address the challenge of validating the trustworthiness of enabling artificial intelligence technologies for future autonomous operations and safety-critical risk management, addressing essential aspects of learning assurance, generalisation, and certification [8]. However, DAA requirements and standards have not yet been defined. Insights from the automotive domain are cautionary; while autonomous vehicle governing strategies include safety, liability, privacy, and cybersecurity, most national governments have only adopted light control-oriented strategies to manage safety risks in the form of non-mandatory testing guidelines. The resulting lack of clarity regarding how liability is apportioned between occupants, manufacturers and other third parties in the event of accidents creates a barrier to adoption [9]. This contrasts with, for example, best practice in ship navigation, with clear specifications on sensor-based hazard detection (as humans cannot see underwater bottom hazards unaided). The International Hydrographic Organisation define the bottom hazard detection requirements (resolution, accuracy, precision) in different water depths and the associated confidence intervals for certification of Electronic Navigation Charts [10]. The required sample density is the discretion of the national authority (e.g. UK Hydrographic Office) but bottom survey equipment such as Multibeam EchoSounder (MBES) must demonstrate capability to detect, for example, 0.5 m³ objects in water depths where under keel clearance is

critical (e.g. port approach lanes) with strict error tolerances. The quantitative benchmarks underpin survey quality assurance and decision making on equipment selection, and enable the validation of new safety-critical software, such as novel ship anti-grounding methods using maritime autonomous surface ships [11]. Similar DAA benchmarks for UAS deployable LiDAR would be beneficial.

B. Data Augmentation for Performance Validation

As computer vision and rule-based approaches to object detection are being displaced by the emergence of deep learning and data-driven Artificial Intelligence (AI) approaches, the availability of labelled and relevant datasets is a key challenge. Annotated datasets like the KITTI Vision Benchmark [12] provide a relatively large amount of labelled camera and LiDAR data for testing automotive object detection software. However, they are inferior to generic image databases such as ImageNet [13] in terms of the quantity of data and the number of labelled classes. Algorithmic data augmentation methods to enhance real-world datasets include Principal Component Analysis [14], handcrafted feature space transformations [15], and modelling the visual context surrounding objects from segmentation annotations [16]. Neural network-based object synthesis and insertion approaches exploiting generative adversarial networks have been applied to automotive [17] and medical imaging [18]. In UAS use cases, distinguishing between birds and other objects is particularly challenging [19]. Successful approaches include Convolutional Neural Networks (CNNs) trained with artificial datasets that insert real UAS and bird images into background videos [20].

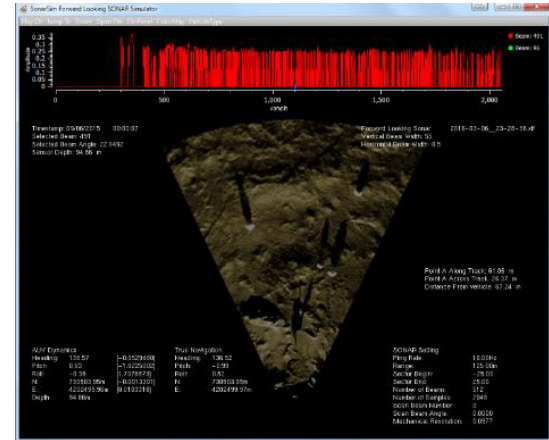


Fig 1. Previous work validated the approach of training SONAR image recognition software with synthetic data in diver detection use cases

Data-driven simulation and digital twinning provides an approach to train and validate safety-critical autonomous vehicle concepts, with successful application in related domains such as autonomous vehicle hazard perception [21]. For instance CARLA's simulation engine has been used to train deep network approaches to autonomous driving employing imitation and reinforcement learning [22]. maritime, Digital Twins of the coastline, port environment and wider marine environment are identified as approaches that will likely become the new digital norm for Maritime Autonomous Surface Vehicle (MASS) navigation [23].

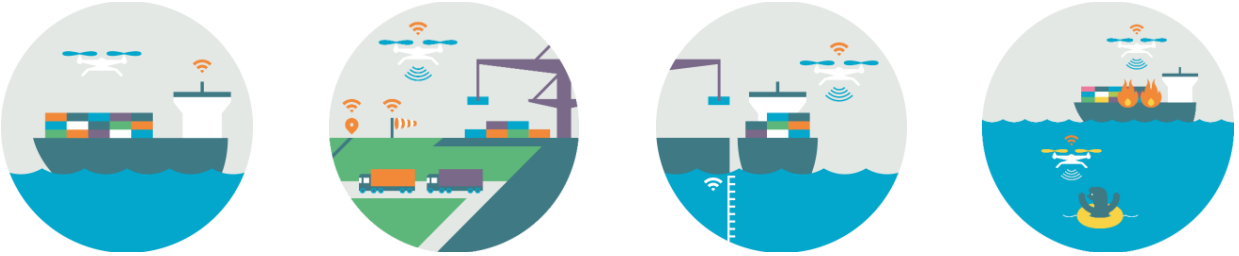


Fig 2. The four RAPID use cases. From left to right, emissions monitoring, infrastructure inspection, ship hull maintenance, incident response

Available UAS perception simulators such as AirSim [24] are built upon game engines such as Unreal and Unity, which have not been validated to represent the dynamic theatre environment at the level of fidelity and resolution required for physically accurate optical propagation and scattering modelling. Replication of LiDAR data artefacts and sensor distortions requires customised geometry processing and compute capability that is beyond the specification of video game and animation rendering engines. However, we have previously demonstrated the potential for exploiting GPGPU ray tracing with custom reflectance modelling and scene geometry optimisation to achieve high-fidelity real-time active sensor simulation in the context of underwater SONAR simulation [25]. The architecture, which is similar to the context of this paper, has been validated in diver threat detection and used to train SONAR image classification algorithms for deployment on autonomous underwater vehicles in ports and harbours [26] (figure 1).

C. Point Cloud Object Detection

Many Neural Network (NN) architectures are capable of detecting classes of objects within point cloud scenes. Early methods focused on building models of indoor scenes, such as the contents of a room, driven by the availability of datasets generated by consumer motion sensing devices such as Microsoft Kinect [27]. Solutions that require pre-processing of the data to build query acceleration structures are less suited to the requirements of real-time performance on embedded hardware. However, recent contributions focusing on automotive applications exhibit high accuracy in cluttered scenes and real-time performance on hardware. Proven NN architectures include PointNet [28] and PointPillar [29]. These offer the potential for re-training improved responses and validation using LiDAR datasets from UAS scenarios, adapting recent approaches in autonomous driving [30].

III. MAINTENANCE INSPECTION USE CASE

A. Risk-aware Autonomous Port Inspection Drones

This work is developed within the H2020 project RAPID (risk-aware autonomous port inspection drones) [31]. RAPID aims to reduce the time and cost of structural condition monitoring of (maritime) transport infrastructure to improve overall transport system safety. Statistically, one in ten bridges across the developed world has a high risk of collapse [32], however current manual approaches to maintenance inspection are exceedingly expensive and slow, requiring the deployment of large crews and multiple vehicles at the asset location over many days. The extended infrastructure downtime during survey operations disrupts commuter traffic and supply chains, a critical issue on intermodal transport systems serving urban industrial hubs. The RAPID project is developing autonomous UAS swarm technology equipped with embedded crack detection software to simplify and accelerate survey operations and enable more frequent condition monitoring of transport system infrastructure. The developed technologies will be embedded in the Port of Hamburg and will validate four priority use cases (see figure 2) involving transport emissions compliance, infrastructure condition monitoring (e.g. bridges), ship maintenance inspection (hulls), and incident response (ship collisions in the coastal zone).

IV. THE RAPID DIGITAL TWIN

The Digital Twin enables the virtual replica of the real world Port of Hamburg situation to be augmented with flourishes of simulated scenarios thus generating synthetic data representative of a wide range of different permutations of hazards, UAS configurations, and LiDAR responses (figure 5). The approach avoids limited datasets and current mainly deterministic approaches for validation in complex situations. The Digital Twin is deployed from two 8-card RTX3090 servers to enable simulation of increased amounts of data.



Fig 3. The RAPID swarm platforms. DJI M300 (left) and XOcean Unmanned Surface Vehicle (right).



Fig 4 Port of Hamburg controlled airspace (top left). Port of Hamburg Digital Twin (top right). Bridges over the Norderlebe, in Google Earth (bottom left). Close view of the Friedensbrücke Bridge, in the Digital Twin (bottom right).

A. Platform and Sensors

The RAPID swarm will combine and extend unmanned aerial and maritime vehicles for operation in the city port of Hamburg. A self-sailing unmanned surface vehicle by XOcean, shown in figure 3, will be adapted to carry a swarm of DJI M300 autonomous unmanned aerial systems. A key safety requirement in the delivery of UAS services in such urban-industrial situations is the capability to detect small sized air collision risks in unsegregated cluttered airspace. As mentioned, the dominant DAA sensor options for UAS are LiDAR, RADAR, and camera, offering a spectrum of value depending on use case requirements.

Table 1. Qualitative metrics for DAA sensors

Sensor Type	Range	Resolution at Range	Depth Accuracy	Penetrating
RGB Camera	Low	Low	Medium (stereo)	No
Thermal	Far	Low	No depth information	No
LiDAR	Medium	Medium	High	No
RADAR	Far	Low	Low	Yes

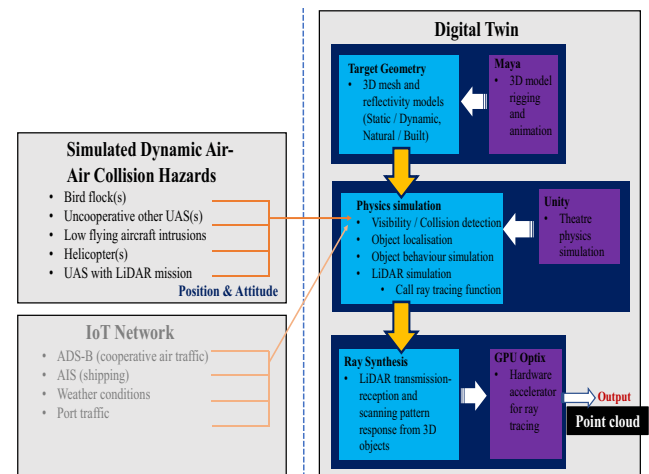


Fig 5. High-level system design.

Table 1 presents a qualitative comparison of DAA sensors. High resolution at medium to far ranges with accurate measurement of depth information is required to allow detection of hazards at and around the built environment and to allow the UAS time to react and perform an avoidance manoeuvre.

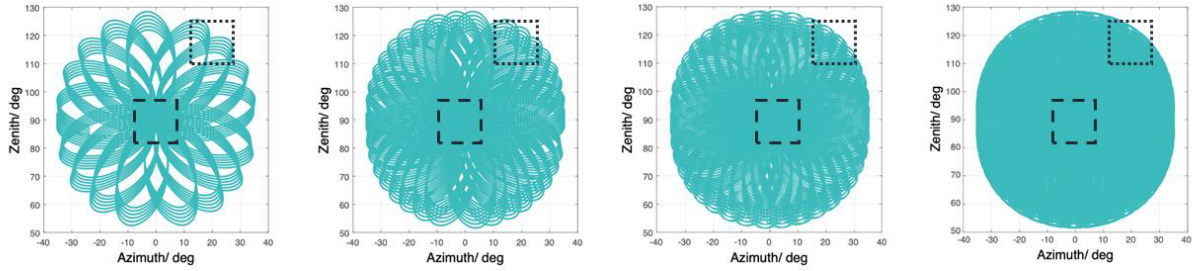


Fig 6. Example of a non-repetitive scanning pattern adapted from the user manual of the Livox Avia, showing the progressive build up in coverage generated over a sequence of scanning iterations. The simulated images in figures 7 and onwards focus on investigate

The capability to penetrate fog, dust, sun glare, etc. offered by active imaging methods is advantageous as it provides robustness to weather. Multi megapixel RGB and thermal cameras are only capable of low resolution at range, and the range of RGB cameras is limited. Both sensor types rely on passive optics and thus have issues with weather, sun, and contrast. LiDAR operates in the visible spectrum, suffering similar weather dependencies as cameras, has medium resolution at range, and due to its active imaging provides scene depth natively. RADAR similarly provides depth information and can overcome weather by penetrating fog, dust, and mist but has poor level of detail. However, in dense and cluttered urban environments, with multiple UAS performing several independent missions in unsegregated airspace, long-range detection technologies will not be as useful as they are in the remote operational scenarios permitted by current regulations. Situations requiring the capability to detect a low-flying aeroplane at a long range are not expected to be frequent events in future urban flight concepts as UAS will operate under 120 m ceilings (or within 15 m clearance of tall structures). In these environments, high-resolution at short-medium ranges will enable better detection capabilities and avoidance manoeuvres in close separation from hazardous entities.

Depth information can be extracted from camera data through software and hardware approaches, and is essential for autonomous navigation and providing a scale reference in simultaneous localization and mapping [33]. However it comes at the expense of considerable additional sensor and/or compute hardware weight. Depth cameras use stereo solutions, relying on stringent mechanical alignment between a pair of horizontally spaced imaging sensors, with depth estimated from the measure of parallax error in the single scene viewed from the two different sensor angles [34]. The computation can be intensive, requiring on-chip calibration to



compensate for vibration and shock and calculation of disparity maps etc. Similarly computational expensive, monocular solutions, rather than triangulating depth from two sensors, use structure from motion and rely on the drone movements to provide the different perspectives over a series of 2D images. Emergent neural network approaches estimate depth perception from vision cues [35].

The combined weight of sensor-compute pairings largely prohibits multi-sensor payload configurations on small-medium UAS, with size, weight, and power constraints being significantly lower compared to automotive and maritime paradigms, and significantly affected by coupling. For example, the M300 energy budget is 550 W, with an unloaded flight endurance of 45 minutes. A typical camera or LiDAR draws only 20-40 W, less than 10% impact on the energy budget. However, with a maximum payload lift capacity of 2.7 kg, of which a camera or LiDAR unit weighs circa 1-2 kg, the mission endurance is reduced to 25 minutes due to the additional trust needed for lift and transport. The achievable endurance is primarily determined by payload weight capacities and not payload power requirements. Embedded companion computers such as the NVidia NX can provide the 21 TFLOPS of compute needed for object detection within a 15 W envelop, but they occupy c. 0.5 kg when housing, cables, and mountings are added to the 0.28 kg board weight. As it is not possible to carry multi-sensor RGB, thermal, LiDAR, and RADAR, with companion computers on the same UAS, equipment selection becomes an exercise in matching the appropriate sensor to the use case requirements. Within RAPID, the capabilities of all systems are being investigated, with this work focusing on establishing the situations where LiDAR is advantageous.



Fig 7. Collections of small flying objects in the Digital Twin sand box (left). Cluttered scene with flock of birds and railway bridge (right).

UAS mountable LiDAR are commercially available and recent advances in sensor miniaturisation have produced integrated units that combine precision mounted LiDAR, IMU, and GNSS into lightweight small form factors. Available instruments are primarily targeted at mapping applications, with most instruments storing data directly to a memory card. However, lightweight versions of automotive variants are becoming available that support real-time interfaces to raw sensor data (e.g. Velodyne Puck Lite) and it is expected that more will become available as regulatory barriers to BVLOS operations are removed and demand for onboard DAA grows.

B. LiDAR Scanning Patterns

LiDAR has fewer controllable parameters than other active imaging sensors. Underwater mapping SONAR and terrestrial RADAR both employ beamforming and interferometric approaches to steer the reception beams. This enables both motion stabilisation, when coupled to an IMU, as well as generation of homogeneously distributed coverage density on complex topography. LiDAR systems on the other hand rely on a rigid emitter-detector laser fan configuration that is mechanically rotated about a fixed axis to sweep a field of view. Repetitive and non-repetitive scanning patterns are possible, however, both produce point clouds with non-uniform densities, with implications for object detection.

Repetitive line scanning is more common in mapping use cases as the fan of lasers is swept repetitively about the roll

axis of the UAS. For example, the VLP-16 scanner head, itself a variant of the HDL-64 employed in self-driving automobiles, is comprised of sixteen lasers in a “fan” of diverging channels, encompassing a 30° vertical field. In mapping modes of operation, the head is oriented such that the fan is mechanically rotated about the UAS alongtrack axis, thus sweeping an acrosstrack swath of bottom detection points. The forward travel of the UAS enables progressive build-up of 3D coverage. The high-frequency pulsing and mechanical scanning can sweep 12 k points through a 360° horizontal field in 100 ms giving 100 m visibility. While the 30° vertical field of view is a limiting factor for airspace DAA use cases, this shortcoming can be approached by mounting the sensor on a tiltable gimbal to sweep a wider vertical sector.

LiDAR scanners (e.g. Livox Avia) that enact a non-repetitive scanning pattern, such as a rotating 5-petal pattern, can illuminate a larger vertical FOV (c. 70-75°). The non-uniform pattern of return pulses produces a dense coverage toward the centre of the FOV but sparser sampling at the outer angles. The capability to detect small objects varies both spatially and temporally, with a latency of up to a second to complete the rotation cycle of the component Risley prisms.

C. LiDAR Simulator

The combination of small perspective-dependent cross-sections and sparse laser sampling of objects such as birds, drones, and small helicopters generates point cloud signatures that can otherwise resemble noise outliers.

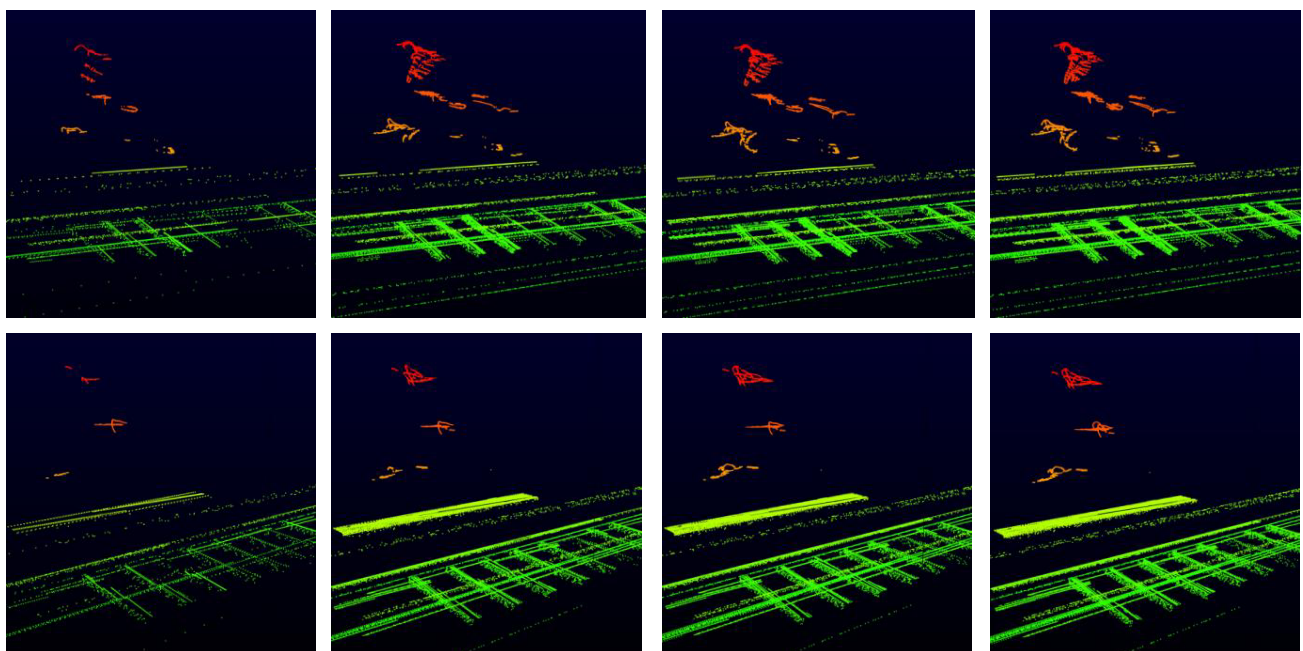


Fig 8. The columns show the cumulative coverage at the 1st, 4th, 8th, and 12th (final) iteration of the LiDAR scanning pattern. At 5m range and centred (top row), the bird shapes are clearly identifiable by the 4th iteration. Alternatively, when image

As a result, they are prone to culling by conventional data cleaning algorithms, rendering them invisible to real-time onboard detect and avoid software. To enable testing of onboard UAS perception software, our validation testbed incorporates data-driven LiDAR simulation to allow evaluation of system responses to unforeseen disturbances and augment pre-designed scenarios with on-demand competency challenges.

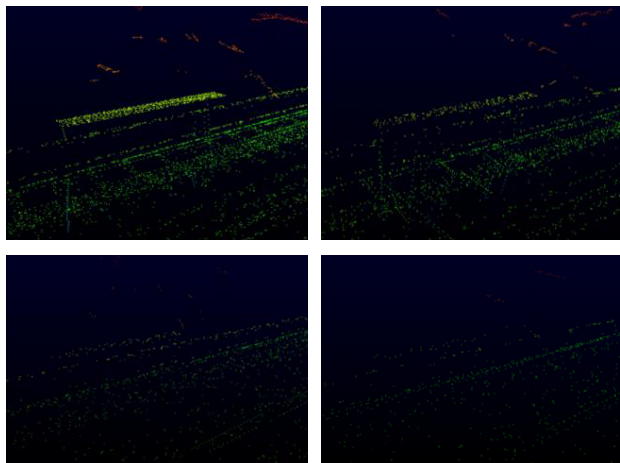


Fig 9. (Top row) The imagery generated on the final iteration of the birds and railway scene at 25m range and at the FOV centre (left), and at the outer periphery (right). (Top row) The situation is repeated for 50m range, at the FOV centre (left), and outer periphery (right).

The virtual replica of the scenario theatre uses Unity to contain the scenario Digital Twin, with models of known built environment structure sourced from a pre-existing virtual replica of Port of Hamburg (figure 4). Unity provides the facility to augment and synchronise the virtual theatre with real-time IoT data from the real-world situation, including live AIS and ADS-B tracking information of known and moving objects such as ships and commercial aircraft. The Digital Terrain Model of the ground is augmented with dynamic simulation of the river Elbe water surface in and around the port lanes, quay walls, berths, and bridges.

Non-cooperative low flying objects (drones, birds, helicopters, and small aircraft) pose an air collision risk and are incorporated into the virtual theatre as scriptable agents (figure 7). The natural object (e.g. birds) synthesis pipeline commences in animation software (Maya), where sequences of keyframe poses corresponding to flight locomotion are generated by skeletal rigging of non-rigid mesh models and cycling through wing movement actions. Inverse kinematics calculates joint rotation and translations of the mesh skin at each keyframe, with smooth motion interpolation between keyframes at simulation runtime. The behaviour and flight profile of all agents, including the host drone, is scriptable in Unity, using waypoint and epoch based missions governed by specifiable dynamic responses and manoeuvrability bounds.

A laser ray tracer is implemented in NVidia Optix to enact the LiDAR simulation and generate the 3D point clouds of objects on accelerated multi-GPU hardware (based on commercial NVidia RTX 3090 cards). The LiDAR ray tracer is modifiable to replicate the known scanning patterns of OEM sensors (figure 6). Data wrappers on the simulator output interface translate navigation and point data into standard protocol formats for interoperability with industry viewers to enable inspection and feature measurement. The data format is augmented to encode object labels generated by the ray trace so that the annotated data can be used to retrain and validate an object detection neural network.

V. RESULTS

Two scenario theatres are virtualised to consider detection of small aircraft and bird flocks. The bird scenario consists of a flock flying across the FOV of the UAS while on approach to a railway bridge. In this instance, the simulation captures the LiDAR data of the scene at three ranges from the centre of the flock bounding box [5 m, 25 m, 50 m]. For each range, the UAS is oriented to illuminate the flock of birds at (a) the centre of the LiDAR FOV and (b) in towards its outer sector, as illustrated in figure 6 by the placement of the long-dash and short-dash boxes respectively. The LiDAR is configured to execute a non-repetitive scanning pattern. Within each of poses described above, a sequence of scan iterations is captured to demonstrate the progressive build-up of coverage and point cloud density. The scanning pattern is a 5 petal flower pattern swept by 5 lasers, which is repeated at 30° increments by rotating the complete about the “view” axis. Thus the complete scanning cycle takes 12 iterations.

The preliminary visual inspection of the generated point clouds in figure 7 demonstrates the progressive accumulation of coverage density as the scanning cycle integrates over successive iterations. While at short range, and in the direct centre of the LiDAR FOV, the object point cloud representations are recognisable as birds after only a few iterations, which translates to a latency of c. 200-300 ms. When imaged at the outer part of the LiDAR FOV, the generated point clouds are significantly sparser and not readily recognisable. Figures 9 demonstrates the LiDAR returns from extended ranges of 25 m and 50 m respectively. Overall, as the range increases the imaging performance degradation is significantly exaggerated, with the point cloud sparsity at 50 m reducing the birds to a few samples and unrecognisable.

The second scenario consists of a small aircraft flying (a) across the FOV and (b) towards the LiDAR. The elevation profile of the aircraft is recognisable at close ranges but begins to break down at 150 m range, especially for the smaller cross-section front profile (figure 10). This is especially problematic as a Cessna 150 at cruise speed (196 km/h) would intercept the UAS within 3 seconds from 150 m range, providing minimal time to react to the air collision risk.

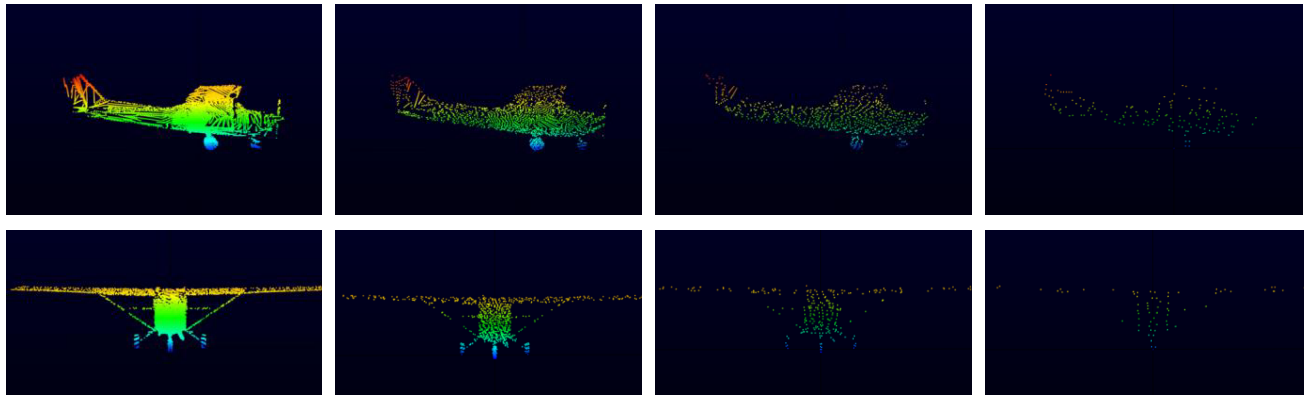


Fig 10. Elevation side profile of a small aircraft imaged at 15 m, 45 m, 75 m, and 150 m (top row, left to right). Elevation front profile of a small aircraft imaged at 15 m, 45 m, 75 m, and 150 m (bottom row, left to right).

Future work is planned to voxelize the LiDAR FOV and use the LiDAR ray tracer to calculate the number of hits per cell generated at different ranges and imaging angles as a prediction of the achievable coverage density. The simulated data will be used to validate the performance of object detection software, and with respect to the inhomogeneous coverage density to help predict the capabilities and vulnerabilities of different LiDAR specifications. In addition, it is planned to use the simulator to generate labelled point and train/retrain the PointNet NN to evaluate its UAS detection capabilities relative to the predicted hits per cell coverage.

VI. CONCLUSIONS

Robust DAA is a prerequisite to achieving fully-autonomous BVLOS operation of UAS. This will not be achieved until autonomous UAS are able to successfully DAA small uncooperative flying objects to avoid collision. LiDAR is a candidate DAA sensor but further investigation is needed to evaluate its capability to tactically sense and detect small air collision risks stemming from small uncooperative aircraft, helicopters, birds, and recreational UAS. This paper presents initial results of using LiDAR simulation to determine and identify detection gaps, with early prototyping focusing on generating the inhomogeneous point clouds characteristics of the spatial-temporal variability of the LiDAR scanning cycle. Our results confirm the challenges in detecting small uncooperative objects (exemplified by birds and small aircraft) as they move through the FOV of the LiDAR sensor and at ranges that provide limited time to react. Our results show that as range increases the imaging performance is degraded, rendering the birds practically unrecognisable at 50m range and even small aircraft becoming sparsely detailed at 150m range.

Future work will extend the scenario Digital Twin so that synthetic data can be generated for training and validating object detection neural networks such as PointNet, to aid the detection of small uncooperative objects at range. The developed platform will be adapted for use during flight planning to identify corner-case restrictions and strategic mitigations to proposed operations with the objective of informing Specific Operational Risk Assessments and LiDAR selection and scanning control during mission flights.

ACKNOWLEDGMENT

The RAPID project is funded through the European Commission's Horizon 2020 research and innovation programme under Grant Agreement number 861211. The authors wish to thank the other consortium partners SINTEF, Thales, Hamburg Port Authority, Fraunhofer CML, XOcean, Revolve, and University of Dundee.

REFERENCES

- [1] NATO, "STO-TR-AVT-278: Considerations for Harmonisation of UAS Regulations for Common NATO Operating Approvals," North Atlantic Treaty Organisation 2020.
- [2] EASA, "Standard scenarios for UAS operations in the 'specific' category," European Union Aviation Safety Agency 2019, Available: <https://www.easa.europa.eu/sites/default/files/dfu/Opinion%20No%20005-2019.pdf>.
- [3] M. U. d. Haag, C. G. Bartone, and M. S. Braasch, "Flight-test evaluation of small form-factor LiDAR and radar sensors for sUAS detect-and-avoid applications," in *2016 IEEE/AIAA 35th Digital Avionics Systems Conference (DASC)*, 2016, pp. 1-11.
- [4] S. Ramasamy, R. Sabatini, A. Gardi, and J. Liu, "LIDAR obstacle warning and avoidance system for unmanned aerial vehicle sense-and-avoid," *Aerospace Science and Technology*, vol. 55, pp. 344-358, 2016/08/01/ 2016.
- [5] X. Yu and Y. Zhang, "Sense and avoid technologies with applications to unmanned aircraft systems: Review and prospects," *Progress in Aerospace Sciences*, vol. 74, pp. 152-166, 2015/04/01/ 2015.
- [6] Y. Liang, Q. Junlong, J. Xiao, and Y. Xia, "A literature review of UAV 3D path planning," in *Proceeding of the 11th World Congress on Intelligent Control and Automation*, 2014, pp. 2376-2381.
- [7] Deloitte, "Unmanned Aircraft Systems (UAS) Risk Management: Thriving Amid Emerging Threats and Opportunities," 2018, Available: <https://www2.deloitte.com/content/dam/Deloitte/us/Documents/public-sector/us-gps-uas-risk-management.pdf>, Accessed on: 22 February 2021.
- [8] EASA, "Artificial Intelligence Roadmap 1.0. A human-centric approach to AI in aviation," 2019, Available: <https://www.easa.europa.eu/sites/default/files/dfu/EASA-AI-Roadmap-v1.0.pdf>.
- [9] A. Taeihagh and H. S. M. Lim, "Governing autonomous vehicles: emerging responses for safety, liability, privacy, cybersecurity, and industry risks," *Transport Reviews*, vol. 39, no. 1, pp. 103-128, 2019/01/02 2019.
- [10] IHO, "S-44, Standards for Hydrographic Surveys," March 2020 2020, Available: https://iho.int/uploads/user/pubs/Drafts/S-44_Edition_6.0.0-Final.pdf.
- [11] J. Riordan, M. Constapel, V. Schneider, and J. Oeffner, "Validation of Ship Anti-Grounding with a Maritime Autonomous Surface Ship in a Distributed Port and Harbour Digital Twin" *Manuscript submitted for publication.*, 2021.

- [12] A. Geiger, P. Lenz, and R. Urtasun, "Are we ready for autonomous driving? the kitti vision benchmark suite," in *2012 IEEE Conference on Computer Vision and Pattern Recognition*, 2012, pp. 3354-3361: IEEE.
- [13] J. Deng, W. Dong, R. Socher, L.-J. Li, K. Li, and L. Fei-Fei, "Imagenet: A large-scale hierarchical image database," in *2009 IEEE conference on computer vision and pattern recognition*, 2009, pp. 248-255: Ieee.
- [14] A. Krizhevsky, I. Sutskever, and G. E. Hinton, "ImageNet classification with deep convolutional neural networks," *Commun. ACM*, vol. 60, no. 6, pp. 84-90, 2017.
- [15] T. DeVries and G. W. Taylor, "Dataset augmentation in feature space," *arXiv preprint arXiv:1702.05538*, 2017.
- [16] N. Dvornik, J. Mairal, and C. Schmid, "Modeling Visual Context is Key to Augmenting Object Detection Datasets," presented at the Proceedings of the European Conference on Computer Vision (ECCV), 2018.
- [17] D. Lee, S. Liu, J. Gu, M.-Y. Liu, M.-H. Yang, and J. Kautz, "Context-aware synthesis and placement of object instances," presented at the Proceedings of the 32nd International Conference on Neural Information Processing Systems, Montréal, Canada, 2018.
- [18] L. Liu, M. Muelly, J. Deng, T. Pfister, and L.-J. Li, "Generative modeling for small-data object detection," in *Proceedings of the IEEE International Conference on Computer Vision*, 2019, pp. 6073-6081.
- [19] A. Coluccia *et al.*, "Drone-vs-Bird Detection Challenge at IEEE AVSS2019," in *2019 16th IEEE International Conference on Advanced Video and Signal Based Surveillance (AVSS)*, 2019, pp. 1-7.
- [20] C. Aker and S. Kalkan, "Using deep networks for drone detection," in *2017 14th IEEE International Conference on Advanced Video and Signal Based Surveillance (AVSS)*, 2017, pp. 1-6.
- [21] A. Amini *et al.*, "Learning Robust Control Policies for End-to-End Autonomous Driving From Data-Driven Simulation," *IEEE Robotics and Automation Letters*, vol. 5, no. 2, pp. 1143-1150, 2020.
- [22] A. Dosovitskiy, G. Ros, F. Codevilla, A. Lopez, and V. Koltun, "CARLA: An open urban driving simulator," in *Conference on robot learning*, 2017, pp. 1-16: PMLR.
- [23] IHO, "The future of Maritime Autonomous Surface Ships (MASS) Navigation," International Hydrographic Organisation2020.
- [24] S. Shah, D. Dey, C. Lovett, and A. Kapoor, "Airsim: High-fidelity visual and physical simulation for autonomous vehicles," in *Field and service robotics*, 2018, pp. 621-635: Springer.
- [25] J. Riordan, F. Flannery, D. Toal, M. Rossi, and G. Dooly, "Interdisciplinary Methodology to Extend Technology Readiness Levels in SONAR Simulation from Laboratory Validation to Hydrography Demonstrator," *Journal of Marine Science and Engineering*, vol. 7, no. 5, 2019.
- [26] F. Caldeira-Saraiva, "Final Report SUPPORT (Security UPgrade for PORTs)," 2015, Available: <https://cordis.europa.eu/docs/results/242/242112/final-published-summary-report-v6.pdf>.
- [27] P. Henry, M. Krainin, E. Herbst, X. Ren, and D. Fox, "RGB-D mapping: Using Kinect-style depth cameras for dense 3D modeling of indoor environments," *The International Journal of Robotics Research*, vol. 31, no. 5, pp. 647-663, 2012.
- [28] R. Q. Charles, H. Su, M. Kaichun, and L. J. Guibas, "PointNet: Deep Learning on Point Sets for 3D Classification and Segmentation," in *2017 IEEE Conference on Computer Vision and Pattern Recognition (CVPR)*, 2017, pp. 77-85.
- [29] A. H. Lang, S. Vora, H. Caesar, L. Zhou, J. Yang, and O. Beijbom, "Pointpillars: Fast encoders for object detection from point clouds," in *Proceedings of the IEEE/CVF Conference on Computer Vision and Pattern Recognition*, 2019, pp. 12697-12705.
- [30] X. Yue, B. Wu, S. A. Seshia, K. Keutzer, and A. L. Sangiovanni-Vincentelli, "A LiDAR Point Cloud Generator: from a Virtual World to Autonomous Driving," presented at the Proceedings of the 2018 ACM on International Conference on Multimedia Retrieval, Yokohama, Japan, 2018. Available: <https://doi.org/10.1145/3206025.3206080>
- [31] RAPID. (February 2021). *Risk-aware Autonomous Port Inspection Drones*. Available: <https://www.rapid2020.eu>
- [32] ASCE, "Infrastructure Report Card," 2017, Available: <https://www.infrastructurereportcard.org/wp-content/uploads/2017/01/Bridges-Final.pdf>.
- [33] M. Rossi, P. Trsljć, S. Sivčev, J. Riordan, D. Toal, and G. Dooly, "Real-time underwater stereofusion," *Sensors*, vol. 18, no. 11, p. 3936, 2018.
- [34] A. O'Riordan, T. Newe, G. Dooly, and D. Toal, "Stereo Vision Sensing: Review of existing systems," in *2018 12th International Conference on Sensing Technology (ICST)*, 2018, pp. 178-184.
- [35] F. Liu, C. Shen, and G. Lin, "Deep convolutional neural fields for depth estimation from a single image," in *Proceedings of the IEEE conference on computer vision and pattern recognition*, 2015, pp. 5162-5170.